NJC

Accepted Manuscript

This is an *Accepted Manuscript*, which has been through the Royal Society of Chemistry peer review process and has been accepted for publication.

Accepted Manuscripts are published online shortly after acceptance, before technical editing, formatting and proof reading. Using this free service, authors can make their results available to the community, in citable form, before we publish the edited article. We will replace this *Accepted Manuscript* with the edited and formatted *Advance Article* as soon as it is available.

You can find more information about *Accepted Manuscripts* in the Information for Authors.

Please note that technical editing may introduce minor changes to the text and/or graphics, which may alter content. The journal's standard Terms & Conditions and the Ethical guidelines still apply. In no event shall the Royal Society of Chemistry be held responsible for any errors or omissions in this *Accepted Manuscript* or any consequences arising from the use of any information it contains.

ROYAL SOCIETY OF CHEMISTRY

www.rsc.org/njc

Journal Name New Journal of Chemistry Dynamic Article Links ►

Cite this: DOI: 10.1039/c0xx00000x

www.rsc.org/xxxxxx

ARTICLE TYPE

Novel nitrogen precursors for electrochemically driven doping of titania nanotubes exhibiting enhanced photoactivity

Katarzyna Siuzdak,*[a] Mariusz Szkoda,[b] Mirosław Sawczak[a] and Anna Lisowska-Oleksiak[b]

Received (in XXX, XXX) Xth XXXXXXXXX 20XX, Accepted Xth XXXXXXXXX 20XX

DOI: 10.1039/b000000x

Nitrogen doped titania nanotubes were successfully sensitized by electrochemical method, i.e. as-anodized titania was immersed in different amine (diethyleneamine-DETA, triethylamine-TEA, ethylenediamine-EDA) and urea (U) solution and a constant potential was applied. The highly ordered morphology of fabricated N-TiO_2 was investigated by using scanning electron microscopy. Spectroscopic techniques, i.e. UV-Vis spectroscopy, Raman spectroscopy, X-ray photoelectron spectroscopy and photoluminescence spectroscopy were utilized to characterize absorbance capability and the crystalline phase, to confirm the presence of nitrogen atoms and to study charge recombination, respectively. The highest photocurrent under both UV-Vis and visible illumination ($\lambda > 420$ nm) was registered for N-TiO_2 sample obtained from diethylenetriamine solution, used as a nitrogen precursor. The photocurrent density exhibited during UV-Vis irradiation by the most active nitrogen doped titania was 2.83 times higher compared to pure TiO_2 nanotubes. The photocatalytic activity studies, demonstrated a significant improvement when N-TiO_2-DETA (52 %) and N-TiO_2-U samples (49 %) where used instead of undoped TiO_2 (27 %). The presented results show that electrochemical doping with 0.5 M amine or urea solutions is a simple, cheap and effective strategy to introduce nitrogen atoms into the titania structure without affecting its morphology.

I Introduction

Titanium dioxide is still one of the most studied materials applied in photocatalytic removal of organic contaminations,[1] hydrogen generation based on the water splitting process,[2] solar cells,[3,4] or self-cleaning surfaces.[5] Nanoparticles are the most common form of TiO_2 material used, but recently we can observe that one-dimensional (1D) Ti-based nanostructures such as nanotubes, nanowires or nanofibers[6] attract extraordinary attention. A significant amount of research in the field of highly-ordered crystalline 1D structures is focused on titania nanotubes that can be easily formed during anodization process when high potential is applied to titanium foil immersed in an electrolyte containing fluorine ions.[7,8] Titania nanotubes exhibit the surface area almost as high as that of porous TiO_2 film; numerous studies support the use of nanotubular structure as suitable for the same applications in which nanoparticles have been typically used.[9] Surprisingly, in the case of the application of titania to processes taking place under illumination, self-aligned nanotubes are expected to exhibit better photoactivity compared to nanoparticles due to their short and undisruptive diffusion path for charge carriers,[10] their structure favoring diffusion of intermediates and the reduced deactivation of photocatalyst in photocatalytic reactions.[11] Although pure titanium dioxide shows low activity under visible light resulting from the wide bandgap energy, many efforts were undertaken to shift the activity towards longer wavelengths in order to expand the compound's applicability under natural solar radiation. To this end, different methods have been proposed in numerous publication, i.e. doping with metal[12] or non-metal[13,14] atoms, sensitization by organic dye,[15] combination with other oxides[16] or deposition of noble metal particles on the oxide surface.[17] The incorporation of non-metal atoms into the structure or onto the surface of the material is still the most popular and effective strategy for enhancing photoactivity.[18] From among many investigated non-metals, nitrogen is regarded as a favorite dopant for titania due to the fact that it is characterized by the atomic size comparable that of oxygen, small ionization energy, metastable center formation and stability.[19] In the case of the doping of ordered titania nanotube array, many approaches have been applied where nitrogen precursor occurs in the gas or liquid phase and sometimes is a component of metal plate subjected to anodization routine. The most common method is calcination of as-prepared nanotubes in a stream of nitrogen[20] or ammonia.[21,22] Despite the fact that gaseous NH_3 used for thermal treatment is still preferred as simple and inexpensive method for nitrogen doping, the environmental regulations which are critical towards hazardous and environmentally unfriendly gaseous chemicals do not support such doping strategy. An additional drawback concerning the application of nitrogen source in the gaseous phase is the production limit of only one type of doped samples during a single thermal annealing process. Another way to incorporate nitrogen atoms is realized by N-ion bombardment at variable angles.[23] Because the multipurpose implanter has to be used, this method is regarded as expensive and sophisticated. As

New Journal of Chemistry Accepted Manuscript

an alternative option, the immersion of as-prepared titania nanotubes in the solution of ammonia[24,25] or hydrazine hydrate[26] for a long time (6-10 hours) followed by thermal annealing in ambient atmosphere was proposed. Other known techniques include a combination of anodization with solvothermal[27] or hydrothermal methods,[28] anodization of Ti-N substrate[26] or anodization in nitrogen-containing electrolyte,[29] liquid phase deposition[30] and thermal annealing in the presence of urea.[31] Recently, nitrogen doping based on electrochemical deposition process was reported; as-prepared TiO_2 nanotubes were immersed in an ammonium chloride solution and steady voltage (1, 2 or 3 V) was applied for 1-3 hours.[32] However, despite usaging of KOH solution as a hole scavenger medium during the photocurrent measurements, the highest current enhancement ratio reported for N-doped titania nanotube arrays was only 30% higher compared to pure TiO_2.

Additionally, it should be noted that some of the doping strategies, besides the introduction of nitrogen atoms into the sample, can possibly affect the tube morphology, i.e. its diameter, length and wall thickness. According to the published literature, annealing in nitrogen[33] or anodization in an electrolyte containing the nitrogen source[34] results in N-doped material whose morphology differs from that of undoped one. Thus, a direct comparison of photoactivity between the pure and modified samples is not reliable as it is well known that the changes in length[35] as well as in tube diameter[36] can significantly impact the material's activity under illumination. In conclusion, a doping method should be simple, inexpensive, and energy efficient, while the applied chemicals can be easily disposed of. Also, the quality of modified samples should be comparable to that of undoped samples, particularly with regard to sample morphology.

In this paper, we propose the electrochemical doping strategy in which post-anodization titanium plate with well-ordered nanotubular structure is immersed in 0.5 M solution of different nitrogen precursors, i.e. three various amines (diethylenetriamine, triethylamine, ethylenediamine) and urea.

The morphology, composition and structure of all the prepared samples were tested using scanning electron microscopy and different spectroscopy techniques, i.e. UV-Vis spectroscopy, Raman spectroscopy, X-ray photoelectron spectroscopy, and photoluminescence spectroscopy. The impact of nitrogen presence was investigated in terms of photocurrents induced at titania electrode that had been immersed in 0.5 M K_2SO_4 and illuminated with a xenon lamp equipped with an AM1.5 filter or, additionally, with a 420 nm cut-off filter in order to examine activity under visible light alone. Furthermore, activity tests towards methylene blue degradation upon exposure to solar simulator radiation allows us to determine the photocatalytic properties of the samples. The relationships between nitrogen precursor type, structural properties, photocurrent and photocatalytic activity were studied and compared.

II Experimental

1 Preparation of nitrogen doped titania nanotubes

Highly ordered titania nanotubes were prepared *via* a two-step electrochemical anodization of Ti plate (Steam, 99.7%) in fluoride-containing solution. Prior to anodization, titanium sheets were ultrasonically cleaned in acetone, ethanol and water (for 10 min. each solvent) and dried under a steam of cold air. The anodization process was performed in a two-electrode configuration, where titanium plate served as an anode and platinum rectangular mesh as a cathode. The distance between the electrodes was kept constant at 2.5 cm. The first anodization took place in the electrolyte containing: 0.27 M NH_4F in 1%/99% v/v water/ethylene glycol solution. During the process, a constant voltage of 40 V was kept for 2 h. The whole anodization process took place in cell with the cooling jacked that keep constant temperature at 23°C (±1°C) using thermostat (Julabo F-12). The same temperature conditions were maintained during all electrochemical processes. Then, the titanium plate was immersed overnight in 0.5% wt. solution of oxalic acid in order to remove pristine rugged nanotube layer. Next, the second anodization was performed on as-cleaned titanium plate under the same conditions as those during the first anodization. After the second anodization, well-aligned pure titania nanotubes were obtained. In order to remove surface debris, titanium plates covered with nanotubes were ultrasonically cleaned in 0.05% wt. HF for 60 s. The preparation of nanotube was realized *via* two stage procedure because it provides better architecture in comparison to single step anodization process. As it was described in many previous reports[37,38,39] after single step anodization random pore arranged surface is obtained. Such process takes place due to random chemical etching by fluoride ions. After removal of this disturbed nanotube oxide layer (i.e. via etching in oxalic acid, using adhesive tape, sonication) a textured substrate with a self-ordered dimples is observed on the metal substrate. During the second anodization process, these concaves serve as nucleation sites for the nanopores formation. Then highly self-ordered TiO_2 nanotube arrays with well-definied top layer can be grown based on the regular nano-patter substrate resulting from the first anodization step. Thus, the first anodization stage could be regarded as a pretreatment of Ti foil surface for proper anodization. Size uniformity and arrangement orderliness facilitate undisturbed charge propagation within the tube that significantly affect, e.g. photocurrent generation.

Nitrogen doping was performed during the next electrochemical process in which the previously prepared titania nanotubes served as an anode and Pt mesh plate as a cathode. The electrolyte used was 0.5 M solution of diethylenetriamine (DETA), triethylamine (TEA), ethylenediamine (EDA) and urea (U). Electrochemical doping was performed at a voltage of 3 V for 1 h. According to the abbreviations used for different nitrogen precursors, the titania nanotube samples were coded as N-TiO_2-DETA, N-TiO_2-TEA, N-TiO_2-EDA and N-TiO_2-U.

Finally, the prepared samples, i.e. pure titania nanotubes and nitrogen doped titania nanotubes were cleaned by sonication in water and then thermally annealed at 450°C for 2 hours, with a heating rate of 2°C min^{-1}. Calcination was performed in order to convert the amorphous titania nanotube layer into the crystalline phase. Thus, the difference in preparation procedure for pure and doped titania nanotubes was only nitrogen doping stage realized by electrochemical process.

2 Characterization

The UV-Vis reflectance and absorbance spectra of titania nanotubes were measured with a dual beam UV-Vis

New Journal of Chemistry Accepted Manuscript

This journal is © The Royal Society of Chemistry [year]

spectrophotometer (Lambda 35, Perkin-Elmer) equipped with diffuse reflectance accessory. The spectra were registered in a range of 300-900 nm, with a scanning speed of 240 nm/min at the room temperature. The Ti foil covered by layer composed of ordered nanotubes was placed in the sample holder dedicated for non-transparent materials. Bandgap value was obtained on the basis of Tauc's plot as the intercept value of the plot of $(\alpha h\nu)^{1/\gamma}$ or $(F(R)\ \nu)^{1/\gamma}$ against light energy ($h\nu$). The values of γ are 1/2, 2, 2/3, 3 for allowed direct, allowed undirect, forbidden direct, and forbidden indirect transition, respectively[40]. For TiO_2 the γ value is ½ because titania is characterized by allow direct band gap. A term called Kubelka-Munk function was used to convert the diffuse reflectance measurements to equivalent absorption coefficient. The following equation was used for transformation:

$$KM = \frac{(1-R)^2}{2R} = \frac{\alpha}{S}$$

Where KM is Kubelka-Munk function, R – the intensity of radiation reflected from the sample, α – absorption coefficient and S is scattering.[41] Described method is commonly applied both for pure[42] and doped[43] titania nanotube arrays.

The Raman spectra were recorded by a confocal micro-Raman spectrometer (InVia, Renishaw) with sample excitation, by means of an argon ion laser emitting at 514 nm operating at 5% of its total power (50 mW).

The scanning electron microscopy (SEM) images of surface and cross-section of pure and nitrogen doped titania nanotube layers were obtained using a scanning electron microscope (EVO-40, Zeiss).

The samples were analyzed by means of X-ray photoelectron spectroscopy (XPS), with the use of a multichamber ultra high vacuum (UHV) system, (Prevac). The investigated samples were not subjected to preliminary chemical treatment prior to analysis. The samples were immobilized on a molibdene holder and degassed at a room temperature until reaching the constant pressure of ~$5 \cdot 10^{-8}$ mbar in the leading lock of the UHV system. Next, the samples were introduced into the analytic chamber of UHV system and subjected to a specific XPS analysis. A monochromatic hemispheric analyser (R4000, VG Scienta) was used as an excitation source. X-ray radiation from Al anode (Kα = 1486.7 eV, U = 12 kV, I = 30 mA) was used. The samples were irradiated with a low-energetic electron source EFG (Electron Flood Gun, E = 2V, 1e = 200 μA) in order to eliminate electrostatic charging of specimens. During the measurements, the vacuum in the analytic chamber was at the level of $8 \cdot 10^{-9}$ mbar or lower. The parameters of XPS spectra registration were as follows: a) for survey spectrum: Pass Energy 200, range: 0 – 1200 eV, step: 0.3 eV, time for single step: 0.4 s, iteration number: 3; b) for a high resolution spectrum: Pass Energy 50, step: 0.1 eV.

The CasaXPS program was used for processing the XPS spectra and the quantitative analysis of the sample surface. In order to normalize spectroscopic measurements, X axis (binding energy, E_{bin}) from XPS spectrum was calibrated for peak characteristics of neutral carbon 1s (E_{bin} = 284.7 eV).

The photoluminescence (PL) measurements were carried out by using a laboratory setup consisting of 0.3 m Czerny-Turner spectrograph (SR303i, Andor) equipped with an ICCD camera (DH740, Andor). Samples were excited with UV LED (365 nm center wavelength, 9 nm FWHM, 350 mW output power). The excitation radiation, focused by quartz lens, was falling on the sample surface at an angle of 45°. Additionally, the band-pass filter (UG11, Schott) was applied between the excitation source and the sample to block UV LED radiation above 380 nm. The fluorescence signal was collected perpendicular to the sample surface using microscope objective and focused on the entrance of optical fiber. In the detection path the band-pass filters (GG44, Schott) were used for blocking the excitation radiation.

3 Photocurrent measurements

The photoelectrochemical performance of pure and nitrogen-doped titania nanotubes was conducted using an AutoLab PGStat 302N potentionstat-galvanostat system (Methrom Autolab) in the standard three-electrode assembly, where titanium foil covered by nanotubes (active surface area of 0.4 cm^2) served as a working electrode, while Ag/AgCl/0.1M KCl and Pt mesh as reference and counter electrodes, respectively. The photoelectrochemical cell was equipped with quartz window and cooling jacket that keep constant temperature at 23°C (±1°C) using thermostat (Julabo F-12). Prior to analysis, 0.5 M K_2SO_4 solution of electrolyte was purged with argon gas for about 1 h. Ar-cushion above the electrolyte was applied during the measurements. The photocurrent measurements were carried out at + 0.5 V *vs.* Ag/AgCl/0.1M KCl bias voltage. A high-pressure 150 W xenon lamp (Osram XBO 150) equipped with AM1.5 filter and the automated light chopper with a period of 20 s was used as a light source. The light intensity was adjusted to 100 mW cm^{-2} (Ophir). In order to perform measurements in the visible light range, the additional cut-off optical filter (λ > 420 nm) was added to the experimental setup.

4 Photocatalytic activity

Photocatalytic efficiency of pure titania and titania doped with nitrogen was determined by studying methylene blue (MB) decomposition in an aqueous solution under a xenon lamp (Osram XBO 150) equipped with AM1.5 filter. The initial MB concentration in a photoreactor of 30 mL capacity was $1 \cdot 10^{-5}$ mol/dm^3. A titanium plate covered by nanotube arrays with the surface area of 3 cm^2 was immersed in methylene blue solution and exposed to irradiation. Prior to illumination, MB solution containing the TiO_2 nanotube layer was kept in the dark for 30 min, allowing the adsorption-desorption equilibrium to be reached. Under constant irradiation, photodegradation of MB was continued for 120 min and the solution was mixed by gas bubbles. The level of light-induced decomposition of MG was determined every 10 min by means of a dual beam UV-Vis spectrophotometer (Lambda 35, Perkin-Elmer).

III Results and disscussion

1 Surface studies

The scanning electron micrographs of the surface of TiO_2 and nitrogen doped titania samples are presented in Fig. 1. Highly ordered and vertically oriented tubes, forming a layer without any cracks, were observed in the as-synthesized pure and doped titania. The nanotube length was determined on the basis of a cross-section image. For both pure and doped nanotubes, the

New Journal of Chemistry Accepted Manuscript

layer thickness was 1.24 μm. The nanotubes were characterized by an average internal diameter of 70 nm and an average wall thickness of 20 nm. Because both pure and doped materials are characterized by the same architecture only the presence of dopant atoms could affect the electrode performance. Such property is very important because the morphology has a great impact on the properties exhibited under illumination, namely, the measured photocurrent[44] and photocatalytic activity.[45,46]

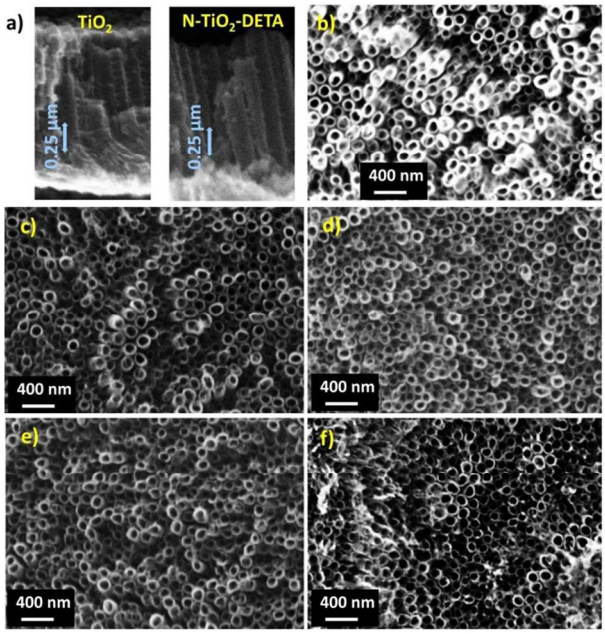

Fig. 1 The scanning electron microscopy images of a) cross-section of pure TiO_2 and N-TiO_2-DETA materials and surfaces of b) pure TiO_2, c) N-TiO_2-DETA, d) N-TiO_2-EDA, e) N-TiO_2-TEA and f) N-TiO_2-U.

2 Investigation of materials structure

In Figures 2a and 2b the absorbance curves and the plot of Kubelka-Munk function *vs*. photon energy (Tauc plot) are presented, respectively. Besides the typical absorption in the UV region, the broad band in the range of 400-650 nm was registered for both pure and nitrogen doped titania. According to Lai et al.,[24] the absorbance at ≤430 nm wavelengths can be attributed to trapped holes, while the strong absorption at ca. 650 nm is caused by trapped electrons. This phenomenon is observed because of the presence of sub-bandgap states resulting from the unusual titania nanotube structure.

In the case of Tauc plot, the intrinsic bandgap of pure and modified TiO_2 was determined by drawing the tangent lines and reading an intercept on photon energy axis. The bandgap energy for pure titania equaled 3.02 eV, whereas for the values of E_{bg} for different nitrogen doped titania were: 2.62 eV (N-TiO_2-TEA), 2.65 eV (N-TiO_2-DETA), 2.88 eV (N-TiO_2-EDA) and 2.90 eV (N-TiO_2-U). For all titania samples treated electrochemically in the nitrogen precursor solution, the bandgap energy was lower compared to pure titania. Such relationship is typical for the nitrogen doped titania nanotube arrays obtained by using different doping strategies.[21,28] The narrowing of bandgap energy is commonly attributed to the interaction between the N2*p* and O2*p* orbital electron states resulting in the activity under visible light.[47] It is also known that nitrogen can form stable oxygen vacancies on the titania surface which leads to visible light photoactivity.[48] Furthermore, a shift in the absorbance edge towards longer wavelength can be attributed to the excitation of electrons from the N2*p* level localized within the bandgap.[49]

It should be also noticed, that bandgap energy of pure titania nanotubes is shifted slightly towards visible range compared to the TiO_2 nanotube film on transparent substrate.[50] This is due to the fact that the barrier layer present at TiO_2 nanotube/Ti substrate interface is characterize by rutile crystalline phase and the nanotube walls consist of anatase crystallites. The bandgap of the rutile is lower (3.0 eV) compared to the anatase (3.2 eV). The rutile phase at the barrier layer leads to the shifting of the absorption edge to higher wavelength. As it was mentioned, last stage of titania nanotube preparation process is thermal annealing in ambient temperature. Then, the diffusion of oxygen take place into the Ti foil. That process occurs according to the second Fick's law and a gradient in the oxide composition along barrier layer is observed. As a consequence, the gradient in the complex permittivity spectrum is created in the oxide layer present below the nanotube array film resulting in light bending before its back reflection from the metal surface. Therefore, when the light is reflected out of the material, its absorption is facilitated and the intensity of the light that left sample is negligible compared to the process that take place in the case of titania nanotube layer deposited on transparent substrate. It was also shown that tube length can significantly affect absorbance of titania nanotube arrays film in visible range despite the fact that TiO_2 is known as material active only under UV illumination.[51] Such high absorption induced by scattering is an important factor that determines the photocatalytic acitivity of titanium dioxide.[52]

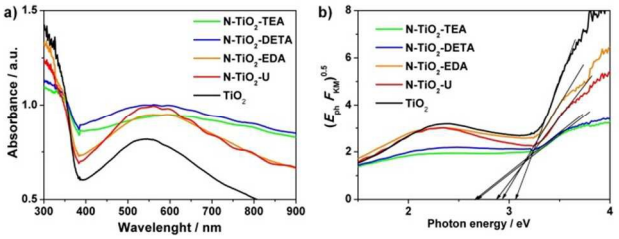

Fig. 2 a) Absorbance spectra and b) the Kubelka-Munk function for pure and doped titania.

Figure 2 shows the Raman spectra of pure TiO_2 and nitrogen doped titania. Five active Raman modes typical of anatase crystalline phase were located at ca. 143, 196, 391, 514 and 634 cm^{-1} and assigned as follows: $E_{g(1)}$, $E_{g(2)}$, B_{1g}, A_{1g} and $E_{g(3)}$.[53] The band corresponding to B_{1g} mode, typically located at 519 cm^{-1}, was hardly visible due to the overlapping of A_{1g} and B_{1g} signals.[54] In general, the Raman spectra recorded for the undoped and nitrogen doped samples were almost identical, which indicates that the material had not changed structurally after the electrochemical treatment in amine- or urea-containing electrolytes. However, it should be noted that the position of $E_{g(1)}$

New Journal of Chemistry Accepted Manuscript

This journal is © The Royal Society of Chemistry [year]

band differed among the samples, reaching the values of 143.13 cm^{-1} (TiO_2), 143.44 cm^{-1} (N-TiO_2-TEA), 143.64 cm^{-1} (N-TiO_2-DETA), 143.46 cm^{-1} (N-TiO_2-EDA) and 143.62 cm^{-1} (N-TiO_2-U). Therefore, due to doping with nitrogen, a slight blue shift of $E_{g(1)}$ band occured. Such displacement of $E_{g(1)}$ signal, attributed to the symmetric stretching vibration of O-Ti-O in TiO_2,[55] can be explained by two factors, i.e. the phonon confinement effect or the non-stochiometry affecting lattice vibrations.[56] According to Choudhury et al.,[57] the generation of oxygen vacancies due to the introduction of dopant atoms will distrib Ti-O-Ti bond resulting in the shifting of $E_{g(1)}$ peak towards higher wavenumbers.

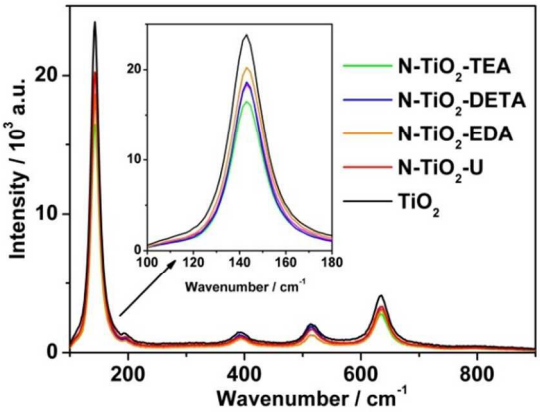

Fig. 3 Raman spectra of pure and nitrogen doped titania.

The presence of nitrogen and the chemical composition of fabricated nanotubes were investigated using X-ray photoelectron spectroscopy. Figure 4 shows the survey spectra of pure and nitrogen doped titania. As an example, the spectra registered for N-TiO_2-DETA are presented. For all the XPS-analyzed materials, the signals typical for Ti, O and C were observed. A band attributable to nitrogen was detected only in samples of doped titania nanotubes. The signal is weak but as it was reported by Isimjan et al.,[58] Li et al.[20] or Yuan et al.,[25] it cannot be neglected. For both TiO_2 and N-TiO_2 materials, the titanium region (see Fig. 5a) was deconvoluted into the Ti2$p_{1/2}$ and Ti2$p_{3/2}$ doublet, corresponding to Ti^{4+} oxidation state. In the case of pure titania, the first and second peak were located at 458.7 eV and 464.4 eV, respectively, whereas for N-doped titania, they were slightly shifted to 458.5 eV and 464.3 eV, respectively. This finding suggests a possible TiO_2 lattice modification by the incorporation of nitrogen.[59]

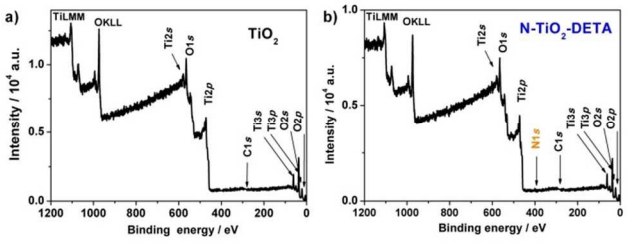

Fig. 4 XPS survey spectrum of a) pure and b) nitrogen doped titania (N-TiO_2-DETA) nanotubes arrays.

The O1*s* spectra obtained for pure and nitrogen doped TiO_2 were deconvoluted into two singlets, i.e. O1*s*A and O1*s*B (see Fig. 5 b). Both oxygen peaks of nitrogen doepd titania at 531.5 eV and 529.8 eV are located at lower energy values compared to the position of O1*s*B (531.7 eV) and O1*s*A (530.1 eV) for pure titania. According to Yuan et al.,[25] the first peak corresponds to Ti-O arrangement, while the second one results from O-H bonding. However, the observed shift may indicate that the introduction of nitrogen atoms into the TiO_2 structure has been achieved.[28]

Apart from titania and oxygen, the signal attributed to carbon was detected in all investigated samples. The carbon C1*s* region (see Fig. 5 c) is formed by three singlets, i.e. C1*s*A, C1*s*B and C1*s*C, with the maxima located at 284.7 eV, 286.1 eV and 288.6 eV, respectively. The highest peak at 284.7 eV orginates from C-C bonds[60] and is typical for graphitic carbon[61] which has been used for calibration of the XPS spectra. According to Isimjan et al.[58] this form of carbon is regarded as a contaminant adsorbed on the titania surface.

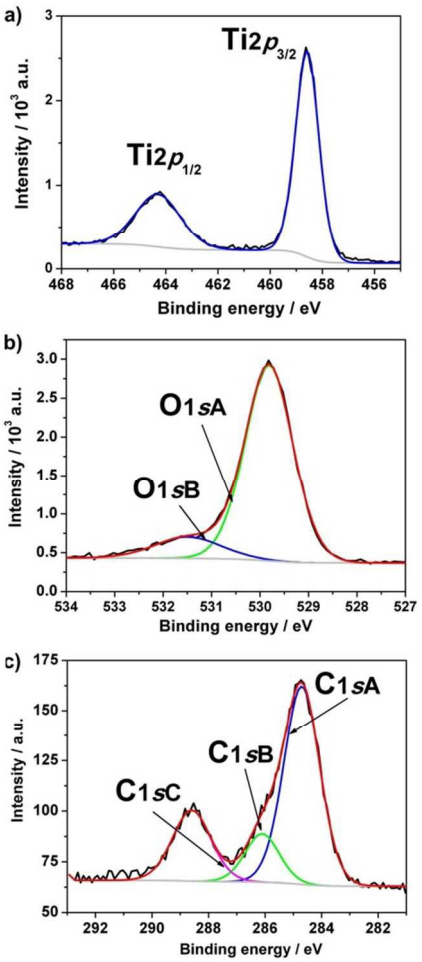

Fig. 5 XPS spectra of a) Ti2*p*, b) O1*s* and c) C1*s* core levels registered for N-TiO_2-DETA.

The singlet at 286.1 eV is assigned to the presence of C-O bond,[62] whereas the last peak located at 288.6 eV suggests the presence

New Journal of Chemistry Accepted Manuscript

of carbon in the form of O-Ti-C bond.[63] It should be noted that the presence of carbon is typical for ordered titania nanotube prepared *via* anodization,[20,28,Error! Bookmark not defined.] and the adventitious hydrocarbon from the XPS instrument. Because anodization took place in an organic electrolyte,[44] carbon could have been introduced into the titania lattice as an additional dopant atom, limiting the effective doping level.

Figure 6 shows the XPS spectra of N1*s* core levels registered for titania nanotubes doped by using tiethyleneamine, diethylenetriamine, ethylenediamine and urea respectively. The nitrogen binding peak obtained from high resolution XPS was deconvoluted into three singlets, i.e. N1*s*A, N1*s*B and N1*s*C, implying the existence of three different types of N states present in all doped samples. The positions and atomic concentration of these signals are listed in Table 1. Similar locations of binding energies characteristic for N were reported by Sun et al.,[28] who applied hydrothermal method with triethylamine as a nitrogen doping strategy. The first signal located in the 397.5 – 397.8 eV range can be attributed to substitional nitrogen in the oxide lattice.[34] According to He et al.[27] nitrogen may also coordinate to the surface of titania. The second band (N1*s*B) close to 400 eV is defined as nitrogen atoms originating from molecularly adsorbed N-containing compounds[20].The third peak is located at 401.8 (N-TiO_2-TEA, N-TiO_2-EDA) or 402 eV (N-TiO_2-DETA, N-TiO_2-U). A similar signal was observed by Lai et al.[24] in nitrogen doped samples before thermal annealing. Some reports attribute the signals at ca. 400 eV and 402 eV to molecular N_2 or NH_3 chemisorbed onto the TiO_2 surface.[64,65] On the other hand, according to Liu et al.,[66] the presence of chemisorbed species is not reasonable because thermal annealing leads to the removal of N_2 and NH_3 via oxidation at elevated temperatures.

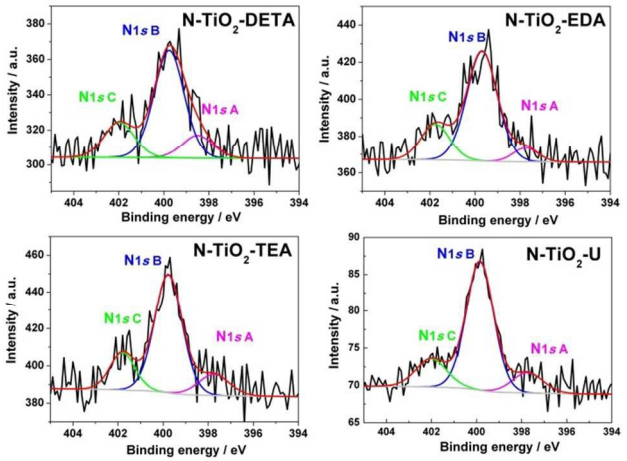

Fig. 6 The N1*s* band from different samples of nitrogen doped titania containing deconvolution signals.

According to other studies, N1*s* located at ca. 400 eV is assigned to O-Ti-N, while the signal present at ca. 402 eV is interpreted as NO like species or Ti-N-O arrangement.[67,68] Based on the work by Liu et al.[66] the nitrogen state in our samples can be regarded as interstitial bonding to titanium or oxygen atoms. However, regardless of its species (i.e. substitional and interstitial form), nitrogen is considered responsible for activity under visible light.[69] As demonstrated in Table 1, the significant differences in atomic concentration of N1*s*A state are present among all doped titania samples. The highest atomic concentration of N1*s*A was reached for N-TiO_2-DETA, whereas the lowest one was observed for N-TiO_2-EDA. Therefore, based on the interpretation of N1*s*A signal, we can conclude that N-TiO_2-DETA contains the highest amount of substitional nitrogen which possibly affects its electrical properties.

Table 1. The position and atomic concentration of nitrogen species present in N-TiO_2 samples.

	N1*s*A position/eV (at.conc. / %)	**N1*s*B** position/eV (at.conc. / %)	**N1*s*C** ***position/eV (at.conc. / %)***
N-TiO_2-U	397.7 (13.3%)	399.8 (67.5%)	401.8 (19.2%)
N-TiO_2-DETA	397.5 (14.2%)	399.8 (64.3%)	402.0 (21.4%)
N-TiO_2-EDA	397.8 (7.4%)	399.7 (70.7%)	401.8 (21.9%)
N-TiO_2-TEA	397.7 (12.5%)	399.9 (70.1%)	402.0 (17.4%)

The atomic concentrations of each element present in the samples are listed in the Table 2. The amount of nitrogen increased in N-doped TiO_2 nanotube samples in an ordered manner, following the sequence of EDA, TEA, U and DETA used as nitrogen sources. As it could be seen, the atomic concentration is low but according to other studies[28,Error! Bookmark not defined.] it could be sufficient to change significantly photoactivity of titanium dioxide. However, the quantification and detailed chemical analysis of small atomic concentration of nitrogen in titania cannot be regarded as fully reliable. Nevertheless, basing on the observed shift in Ti2*p* and O1*s* signals for doped TiO_2 in comparison to pure titania and the nature of $N1_s$ signal observed only for doped materials we can conclude that nitrogen atoms were successfully introduced into the titania nanotube array using electrochemical doping strategy.

Table 2. The atomic composition of pure and doped materials estimated on the basis of XPS spectra.

	Ti / at.%	**O / at.%**	**C / at.%**	**N / at.%**
N-TiO_2-TEA	23.37	60.01	15.36	**0.63**
N-TiO_2-DETA	24.60	60.30	14.00	**1.10**
N-TiO_2-EDA	24.79	58.51	15.79	**0.46**
N-TiO_2-U	25.10	59.30	14.60	**1.00**
TiO_2	25.00	60.30	14.70	**0**

Photoluminescence emission spectroscopy is widely used for examination the quenching efficiency of charge carrier to understand the destiny of electron-hole pairs in semiconductor as *PL* emission results from the recombination of free charge carriers.[70,71] Photoluminescence spectra of pure titania nanotubes and nitrogen doped samples are presented in Fig. 7. In general, the PL intensity for doped titania was lower compared to pure TiO_2 nanotubes, reaching its minimum for N-TiO_2-DETA. The observed tendency indicates that the charge separation rate resulting from nitrogen doping is more efficient, while the

New Journal of Chemistry Accepted Manuscript

This journal is © The Royal Society of Chemistry [year]

radiative recombination is inhibited. Photoluminescence spectra of pure titania nanotubes and nitrogen doped samples are presented in Fig. 7. In general, the PL intensity for doped titania was lower compared to pure TiO_2 nanotubes, reaching its minimum for N-TiO_2-DETA. The observed tendency indicates that the charge separation rate resulting from nitrogen doping is more efficient, while the radiative recombination is inhibited.

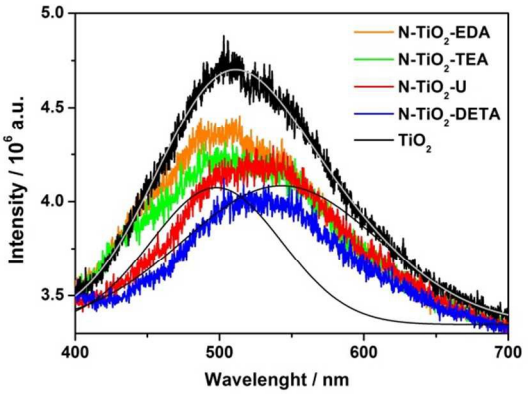

Fig. 7 Photoluminescence spectra of pure and N-doped samples. As an example a deconvolution for pure TiO_2 spectra was shown.

Because charge transport and PL intensity are closely related, radiative recombination occurs when the mobile and trapped charges spatially overlap. We can predict that charge generated in nitrogen doped samples under illumination will not be effectively quenched. Therefore, besides the improved absorbance capabilities of N-doped TiO_2, a less disturbed path for charge percolation can affect the enhancement of registered photocurrent. Detailed analysis of recorded signals allows to conclude that in the case of TiO_2, N-TiO_2-EDA and N-TiO_2-TEA materials, spectrum consists of two signals as it was reported by Wang et al.[72]. As an example, for undoped titania two constituent peaks were shown. The first one is located at 495 eV and the second one is present at 540 eV which could be attributed to the transition from the oxygen vacancies with two trapped electrons and one trapped electron to the valence band, respectively[67]. In the case of N-TiO_2-U and N-TiO_2-DETA the shape of spectra is different comparing to other materials. The peak is wide with a maximum located at about 530 nm. According to Forss et al.[73] PL located around 530 eV band can be attributed to the surface states whereas according to Redmond et al.[74] it can be regarded as an intraband surface state of the nanocrystalline anatase film associated with the Ti atoms (adjacent to oxygen vacancies) at the surface. On the contrary, according to the exciton dynamics model proposed by Jang et al.,[75] the observed signal fits the energy level at which deep trapped excitons can be located. The absence of clear signal at lower energies could indicate that transition from the oxygen vacancies with two trapped electrons does not take place. Furthermore, as it was described by Prokes et al.[76] the change in the shape of photoluminescence spectra due to the doping procedure results from change of surface environment. Thus, application of diethyelnetriamine and urea as nitrogen precursor could introduce some surface localized defects.

3 Photoelectrochemical properties

The photoelectrochemical behavior of pure and nitrogen doped TiO_2 electrodes exposed to radiation from a solar simulator equipped with an AM1.5 filter is presented in Fig. 8. The photocurrent densities in all examined samples increased with increasing potential applied to the photoanode. In the case of the two best performing N-doped samples (N-TiO_2-DETA and N-TiO_2-U), the saturated photocurrent was almost three times higher in comparison to that generated at the electrode composed of pure titania nanotubes. In order to investigate photoelectrode stability, the current was measured at 0.5 V bias voltage for 10 min. Figure 9 shows the transient photocurrent response of pure and nitrogen doped TiO_2 nanotube arrays by on-off cycles registered under UV-Vis and Vis irradiation. The graph illustrates how the current rapidly increased and decreased when the radiation is switched on and off, respectively. The values of photocurrent density registered after 500 s of measurement under different light conditions, and the photocurrent ratios between the doped TiO_2 and pure TiO_2 photoelectrodes are presented in Table 3.

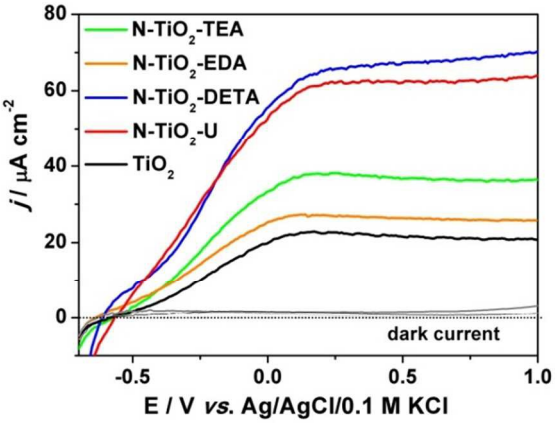

Fig. 8 Linear voltamperogram of pure and nitrogen doped TiO_2 nanotubes immersed in 0.5 M K_2SO_4 (scan rate 20 mV/s).

The net photocurrent density was calculated by substracting the dark current density from the respective current measured under illumination; the dark current densities were negligible for all samples tested. As shown in Fig. 9 and in Table 3, the saturated current density of all nitrogen doped titania nanotube photoelectrodes under both UV-Vis and Vis irradiation was higher compared to undoped photoelectrode.

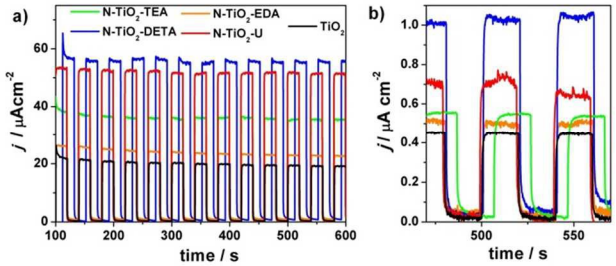

Fig. 9 Transient photocurrent response of pure and nitrogen doped TiO_2 nanotubes at 0.5 V *vs.* Ag/AgCl/0.1 M KCl under

New Journal of Chemistry Accepted Manuscript

UV-Vis and Vis illumination.

However, the highest photocurrent was observed for N-TiO_2-DETA reaching 55.8×10^{-6} A cm^{-2} and 10.8×10^{-7} A cm^{-2} under UV-Vis and Vis illumination, respectively. The aforementioned photocurrents were 2.83 and 2.5 times higher than the current registered for undoped TiO_2 under the same light conditions. The enhancement in the light-induced current density in N-doped sample resulted from the narrower bandgap energy as compared to undoped sample. As demonstrated in the photoluminescence description, nitrogen doped titania is characterized by lower luminescence compared to pure titania, which indicates a reduction in the recombination processes of photogenerated charge under UV light. Despite the fact that N-doped titania is characterized by higher absorbance in the visible region than pure TiO_2, the rather low values of I_{ph}(Vis) could result from the enhanced recombination at the impurity sites when sample is irradiated with Vis light alone.[77]

Table 3. The photocurrent values registered for undoped and nitrogen doped TiO_2 under Vis and UV-Vis illumination after 500 s of measurement. For each photoelectrode, the photocurrent ration between the doped TiO_2 and pure TiO_2 is given in the brackets.

material	I_{ph} UV-vis / 10^{-6} A cm^{-2}	I_{ph} vis/ 10^{-7} A cm^{-2}
N-TiO_2-TEA	36.3 (× 1.84)	5.5 (× 1.2)
N-TiO_2-DETA	**55.8 (× 2.83)**	**10.8 (× 2.5)**
N-TiO_2-EDA	23.7 (× 1.20)	5.0 (x 1.3)
N-TiO_2-U	51.8 (× 2.63)	7.4 (x 1.7)
TiO_2	19.7	4.3

Additionally, the values of current densities for various titania samples differs significantly despite the fact that doping process was performed in the same concentration of nitrogen precursor. Therefore, the nature of nitrogen source affecting the interaction with titania nanotube structure should be responsible for properties of obtained material. Similar behaviour was observed when other nitrogen sources with same concentration or Ti/N ratio were used for solvothermal synthesis[78], microwave assisted hydrothermal growth[79], or modified sol-gel synthesis[80] of N-TiO_2 nanomaterials. It is very likely that observed higher photoactivity is achieved due to chemical structure of the used precursor (see figure 10).

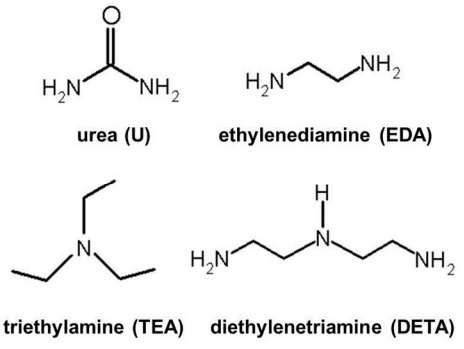

Fig. 10 Chemical structures of nitrogen precursors.

The urea (U) has a carbonyl group flanked by two primary amines, ethylenediamine (EDA) is a primary amine with two amine groups, triethylamine (TEA) has three alkyl branches and is considered a tertiary amine, diethylenetriamine (DETA) is a secondary amine with two alkyl branches terminated with amine groups. It should be also noted that chemicals contain different number of nitrogen atoms per one molecule. As it was mentioned by Ananpattarachai et al.[80]and Lin et al,[81] mentioned dissimilarities in the basic character of the nitrogen precursor can cause significantly different characteristics and properties of each N-doped TiO_2 that consequently alter the photocatalytic activity of the materials. This is our preliminary assumption and we would like to stress that without further studies concerning mechanism of doping process ultimate conclusions are not possible to be withdrawn.

4 Photocatalytic properties

The photocatalytic activity of pure and nitrogen doped titania nanotubes was investigated on the basis of degradation progress of a commonly used model pollutant, i.e. methylene blue (MB) under illumination generated by a xenon lamp equipped with an AM 1.5 filter. As presented in Fig. 11, the lowest degradation rate of methylene blue occured when no catalyst was added (blank sample). The efficiency of MB decomposition significantly improved after the application of photocatalyst, i.e. titanium plate covered by TiO_2 nanotubes. The photocatalytic measurements carried out without the catalyst sample (blank probe) and with the application of pure TiO_2 are regarded here as a reference. Methylene blue present in the blank sample absorbed the visible light therefore degradated under illumination.[20] After a 2-h illumination in the presence of plate covered with pure titania nanotubes, the degradation of methylene blue reached 27%. From among all tested samples, the highest degradation efficiency of 52% was observed for N-TiO_2-DETA. In the case of other nitrogen doped TiO_2 samples, the efficiency was slightly lower and equaled 37, 38 and 49% for N-TiO_2-TEA, N-TiO_2-EDA and N-TiO_2-U, respectively.

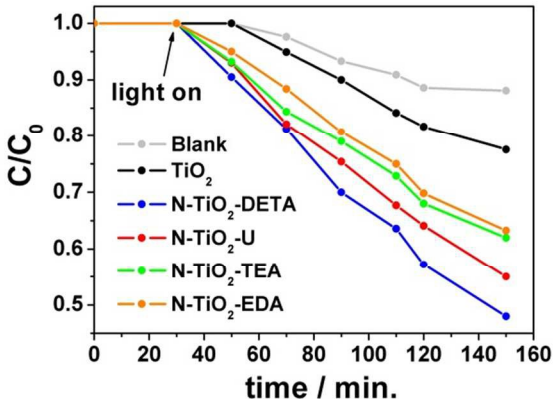

Fig. 11 The progress of methylene blue degradation in the presence of N-doped and undoped titania nanotube arrays layer under solar simulator radiation.

The sequence from the most photoactive to the least photoactive nitrogen-doped titania nanotubes corresponds to the sequence from the highest photocurrent to the lowest photocurrent under

New Journal of Chemistry Accepted Manuscript

This journal is © The Royal Society of Chemistry [year]

both UV-Vis and Vis illumination. It is apparent that the degradation of methylene blue has significantly improved due to the doping of titania nanotubes with nitrogen. Such enhanced activity can be attributed to: improved absorbance capability in the visible range, more effective charge separation and charge transport.

The photodegradation of methylene blue can be fitted into a first-order exponential decay function: $\ln(C/C_0) = -kt$ where k is the first-order kinetic constant (see Fig. 12). According to the model, N-TiO_2-DETA sample exibited the highest constant rate of 6.6×10^{-3} min.$^{-1}$, while the rate for pure titania was constant and almost three times lower (2.3×10^{-3} min.$^{-1}$).

Based on the analysis of material characteristics and the measurements of photocurrent and photocatalysis, it has been established that the enhancement of activity under illumination is strongly related to the presence of nitrogen in doped materials. According to Cheng et al.,[82] incorporation of nitrogen species leads to the formation of new energy levels resulting in a decrease in the bandgap energy value compared to pure TiO_2. Additionally, such impurity levels can act as trapping sites where efficient charge separation occurs.[83] When a sample is exposed to visible light, the electron transfer is facilitated from N2*p* energy states towards the conduction band. Simultaneously, the transport of electrons can be realized through surface states towards titanium metal plate serving as a back contact. The holes remaining in the valence band react with the adsorbed H_2O, O_2 or OH^- molecules and then the generation of highly active species such as OH radicals and peroxo ions is initiated.[25] Such oxidable species are directly involved in the decomposition pathway of organic contaminants (e.g. methylene blue).

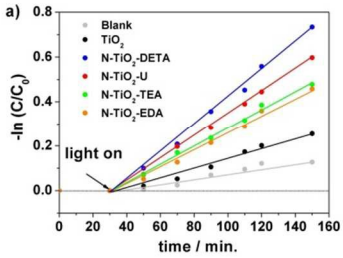

sample	kinetic constant k / 10^{-3} min^{-1}
blank	1.3
TiO_2	2.3
N-TiO_2-EDA	4.2
N-TiO_2-TEA	4.4
N-TiO_2-U	5.6
N-TiO_2-DETA	6.6

Fig. 12 a) The kinetics of MB degradation in the presence of pure and N-doped TiO_2 used as a photocatalys, b) Kinetic constants of MB degradation carried out without a photocatalyst (blank sample) and with pure and nitrogen doped titania nanotubes.

As it could be seen, the difference between various nitrogen doped titania in their photoactivity measured as photocatallytic efficiency and photocurrent is not the same. This phenomenon results from different nature and mechanism of current generation and degradation process carried out under illumination. In the case of photocurrent measurement, voltage is applied to the irradiated electrode and supports the charge dissociation within the material. On the other hand, during photocatalysis measurements only light has impact on the degradation progress. Therefore, efficient separation of hole and electron is not such efficient process as in the case of photocurrent measurement. Similar lack of correlation between activities during photocurrent and photocatalytic degradation using nitrogen doped titania nanotubes was described by Yuan et al.[25] or Sun et al.[28] Thus, the photoactivity measured as photocurrent and photodegradation efficiency cannot be directly compared.

IV Conclusions

The electrochemical doping strategy was proposed to fabricate N-doped titania nanotubes by using three different types of amines (diethylenetriamine, triethylamine, ethylenediamine) and urea as nitrogen source. The basic principle of the proposed method is based on the immersion of as-anodized Ti-plate covered with nanotube arrays in 0.5 M amine or urea solution and the application of constant voltage. After thermal annealing, all samples were characterized as an anatase crystalline phase by means of Raman spectroscopy. As illustrated by scanning electron microscopy images, the obtained materials formed crack-free layers composed of highly-ordered, vertically-oriented tubes, 1.24 μm in length and with an internal diameter of 70 nm. The presence of nitrogen in all doped materials was confirmed by X-ray photoelectron spectroscopy studies. Furthermore, it was found that presence of nitrogen resulted in the narrowing of bandgap energy and in a decrease in photoluminescence intensity. Both the steady-state photocurrent and the photocatalytic measurements showed that nitrogen doped TiO_2 is much more active than pure titania, i.e. the best performing N-TiO_2 material obtained fromdiethylenetriamine solution exhibited 2.83 and 2.5 times higher photocurrent under UV-Vis and Vis illumination, respectively, as compared to pristine titania. Thus, diethylenetriamine can be regarded as a new, promising precursor used for nitrogen doping of titania nanotube. In conclusion, the described electrochemical doping strategy is a facile, simply and effective way to obtain doped TiO_2 characterized by highly enhanced photoactivity. Because nitrogen doping was realized during short, inexpensive electrochemical process and disposal of liquid chemicals is easier than gaseous nitrogen precursors (e.g. ammonia), proposed doping strategy could be successfully applied for technological scale, e.g. for preparation of photoelectrodes used for water spitting or degradation of organic pollution under sun radiation. Further studies concerning mechanism of doping process will be carried out in order to explain the impact of precursor nature on the enhancement of titania photoactivity.

Notes

[a] *Centre for Plasma and Laser Engineering, The Szewalski Institute of Fluid Flow Machinery, Polish Academy of Science, Fiszera 14, Gdansk 80-231, Poland Address, Address, Town, Country. Fax: +48 58 3416144; Tel: +48 58 6995294; *E-mail: ksiuzdak@imp.gda.pl*

[b] *Department of Chemistry and Technology of Functional Materials, Chemical Faculty, Gdansk University of Technology, Narutowicza 11/12, Gdansk 80-233, Poland*

Acknowledgements

This work was financially supported th ePolish National Science Center: Grant No 2012/07/D/ST5/02269).

References

New Journal of Chemistry Accepted Manuscript

1 I.K Konstantinou and T.A. Albanis, *Appl. Catal. B,* 2004, **49**, 1.
2 M. Ye, J. Gong, Y. Lai, C. Lin and Z. Lin, *J. Am. Chem. Soc.* 2012, **134**, 15720.
3 G. K. Mor, K. Shankar, M. Paulose, O.K. Varghese and C.A. Grimes, *Nano Lett.* 2006; **6**, 215.
4 K. Siuzdak, M. Abbas, L. Vignau, M. Devynck, G.V. Dubacheva and A. Lisowska-Oleksiak, *J. App. Phys.* 2012, **112**, 123110.
5 B. Tryba, M. Piszcz and A.W. Morawski, *The Open Mater. Sci. J.* 2010, **4**, 5.
6 W. Zhou, H. Liu, R.I. Boughton, G. Du, J. Lin, J. Wang and D. Liu, , *J. Mater. Chem.* 2010, **20**, 5993.
7 B. Chen, J. Hou and K. Lu, *Langmuir* 2013, **29**, 5911.
8 D. Kowalski, D. Kim and P. Schmuki, *Nano Today* 2013, **8**, 235.
9 J.M. Macak, H. Tsuchiya, A. Ghicov, K. Yasuda, R. Hahn, S. Bauer and P. Schmuki, *Curr. Opin. Solid State Mater. Sci.* 2007, **11**, 3.
10 Y, Zhang, D. Wang, S. Pang, Y. Lin, T. Jiang and T. Xie, *Appl. Surf. Sci.* 2010, **256**, 7217.
11 I.S. In, M.G. Nielsen, P.C.K. Vesborg, Y.D. Hou, B.L. Abrams, T.R. Henriksen, O. Hansen and I. Chorkendorff, *Chem. Commun.* 2011, **47**, 2613.
12 T. Mishra, L.; Wang, R. Hahn and P. Schmuki, *Electrochim. Acta* 2014, **132**, 410.
13 A. Subramanian and H.W. Wang, *Appl. Surf. Sci.* 2012, **258**, 6479.
14 A. Lisowska-Oleksiak, K. Szybowska, and V. Jasulajtiene, *Electrochimica Acta* 2010, **55**, 5881.
15 M. Paulose, K. Shankar, O.K. Varghese, G.K. Mor and C.A. Grimes, *J. Phys. D: Appl. Phys.* 2006, **39**, 2498.
16 M. Wang, L. Sun, Z. Lin, J. Cai, K. Xie and C. Lin, *Energy Environ. Sci.* 2013, **6**, 1211.
17 K. Siuzdak, M. Sawczak, M. Klein, G. Nowaczyk, S. Jurka and A. Cenian, *Phys. Chem. Chem. Phys.* 2014, **16**, 15199.
18 Y.C. Nah, I. Paramasivam and P. Schmuki, *Chem. Phys. Chem.* 2010, **11**, 2698.
19 D. Lu, M. Zhang, Z. Zhang, Q. Li, X. Wang and J. Yang, *Nanoscale Res. Lett.* 2014, **9**, 272-280.
20 Q. Li and J. K. Shang, *Environ. Sci. Technol.* 2009, **43**, 8923.
21 S. In, P.C.K. Vesborg, B.L. Abrams, Y. Hou and I. Chorkendorff, *J. Photochem. Photobiol. A Chem.* 2011, **222**, 258.
22 S. Zhang, F. Peng, H. Wang, H. Yu, S. Zhang, J. Yang and H. Zhao, *Catal. Comm.* 2011, **12**, 689.
23 A. Gihcov, J.M. Macak, H. Tsuchiya, J. Kunze, V. Haeblein, L. Frey and P. Schmuki, *Nano Lett.* 2006, **6**, 1080.
24 Y.K. Lai, J.Y. Huang, H.F. Zhang, V.P. Subramaniam, Y.X. Tang, D.G. Gong, L. Sundar, L. Sun, Z. Chen and C.J Lin, *J. Hazard. Mater.* 2010, **184**, 855.
25 B. Yuan, Y. Wang, H. Bian, T. Shen, Y. Wu and Z. Chen, *Appl. Surf. Sci.* 2013, **280**, 523.
26 J. Xu, Y. Ao, M. Chen and D. Fu, *Appl. Surf. Sci.* 2010, **256**, 4397.
27 Z. He, W. Que, Y. He, J. Hu, J. Chen, H.M.J. Javed, Y. Ji, X. Li and D. Fei, *Ceram. Intern.* 2013, **39**, 5545.
28 L. Sun, J. Cai, Q. Wu, P. Huang, Y. Su and C. Lin, *Electrochim. Acta* 2013, **108**, 525.
29 K. Shankar, K.C. Tep, G.K. Mor and C.A. Grimes, *J. Phys. D: Appl. Phys.* 2006, **39**, 2361.
30 J. Wang, Z. Wang, H. Li, Y. Cui and Y. Du, *J. Alloys Comp.* 2010, **494**, 372.
31 S. Liu, L. Yang, S. Xu, S. Luo and Q. Cai, *Electrochem. Comm.* 2009, **11**, 1748.
32 S. Li, S. Lin, J. Liao, N. Pan, D. Li and J. Li, *Int. J. Photoenerg.* 2012, id 794207, doi: 10.1155/2012/794207.
33 P. Xiao, D. Liu, B.B. Garcia, S. Sepehri, Y. Zhang and G. Cao, *Sens. Actuat. B* 2008, **134**, 367.
34 R.P. Antony, T. Mathews, K. Panda, B. Sundaravel, S. Dash and A.K. Tyagi, *J. Phys. Chem. C* 2012, **116**, 16740.
35 R. Beranek, J.M. Macak, M. Gartner, K. Meyer and P. Schmuki, *Electrochim. Acta 2009*, **54**, 2640.
36 A. Atyaoui, H. Cachet, E.M.M. Sutter and L., Bousselmi, *Surf. Inter. Anal.* 2013, **45**, 1751.
37 G.D. Sulka, J. Kapusta-Kołodziej, A. Brzóska and M. Jaskuła, *Electrochim. Acta* 2013, **104**, 526.
38 W. Wei, G. Oltean, C.W. Tai, K. Edstrom, F. Bjorefors and L. Nyholm, *J. Mater. Chem. A* 2013, **1**, 8160.
39 S. Li, G. Zhang, D. Guo, L. Yu and W. Zhang, *J. Phys. Chem. C* 2009, 113, 12759.
40 D.V. Bavykin and F.C. Walsh, Titanate and titania nanotubes, Synthesis, Properties and Application, *RSC Publishing,* 2010.
41 A. Furube, T. Asahi, H. Masuhara, H. Yamashita and M. Anpo, *J. Phys. Chem. B* 1999, **103**, 3120.
42 A. Bjelajaca, V. Djokicb, R. Petrovicb, G. Socolc, I.N. Mihailescuc, I. Floread, O. Ersend and D. Janackovic, *Appl. Surf. Sci*. 2014, **309**, 225.
43 R.P. Antony, T. Mathews, P.K. Ajikumar, D. Nandagopala Krishna, S. Dash and A.K. Tyagi, *Mater. Res. Bull.* 2012, **47**, 4491.
44 L. Tsui, T. Homma and G. Zangari, *J. Phys. Chem. C* 2013, **117**, 6979.
45 H. Zhuang, C. Lin, Y. Lai, L. Sun and J. Li, *Environ. Sci. Technol.* 2007, **41**, 4735.
46 D. Wang, Y. Liu, B. Yu, F. Zhou and W. Liu, *Chem. Mater.* 2009, **21**, 1198.
47 R. Asahi, T. Morikawa, T. Ohwaki, K. Aoki and Y. Taga, *Science* 2001, **293**, 269.
48 X. Song and L. Gao, *Langmuir* 2007, 23, 11850
49 Y. Su, X. Zhang, M. Zhou, S. Han and L. Lei, *J. Photochem. and Photobiol. A: Chem.* 2008, **194**, 152.
50 C.A. Grimes and G.K. Mor, TiO_2 Nanotube Arrays, Synthesis, Properties, and Applications, Springer 2009.
51 K.G. Ong, O.K Vargheseand G.K Mor and CA Grimes, *J. Nanosci. Nanotechnol.* 2005, **5** ,1.
52 H. Yaghoubi, Z. Li, Y. Chen, H. T. Ngo, V. R. Bhethanabotla, B. Joseph, S. Ma, R. Schlaf and A. Takshi*, ACS Catal.* 2015.**5** .327.
53 X. Chen and S S. Mao, *Chem. Rev.* 2007, **107**, 2891.
54 S.W. Kim, R. Khan, T.J. Kim and W.J. Kim, *Bull. Korean Chem. Soc.* 2009, **29**, 1217.
55 F.D. Hardcastle, *J. Arkansan Acad. Sci.* 2011, **65**, 43.
56 Q. Liu, D. Ding and C. Ning, *Materials* 2014, **7**, 3262.
57 B. Choudhury, M. Dey and A. Choudhury, *Inter. Nano Lett.* 2013, **3**, 25.
58 T.T. Isimjan, A. El Ruby, S. Rohani and A.K. Ray, *Nanotechnology* 2010, **21**, 055706.
59 Y.Y. Chen, S.M. Zhang and Y. Yu, *J. Dispers. Sci. Technol.* 2008, **292**, 245.
60 K. Nagaveni, G. Sivalingam, M.S. Hegde and G. Madras, *Appl. Catal. B Environ.* 2004, **48**, 83.
61 P. Srinivasu, A. Islam, S.P. Singh, L. Han, M.L. Kantam and S.K. Bhargava, *J. Mater. Chem.* 2012, **22**, 20866.
62 Q. Wang, D. Yang, S. Chen, Y. Wang and Z. Jiang, *J. Nanopartic. Res.* 2007, **9**, 1087.
63 X.Y. Hu, T.C. Zhang, Z. Jin, W. Xu, J. Yan, J.P. Zhang, L.D. Zhang and Y.C. Wu, *Mater. Lett.* 2008, **62**, 4579.
64 T. Horikawa, M. Katoh and T. Tomida, *Microporous Mesoporous Mater*. 2008, **110**, 397.
65 J.H. Xu, W.L. Dai, J.X. Li, Y. Cao, H.X. Li, H.Y. He and K.N. Fan, *Catal. Commun.* 2008, **9**, 146.
66 H. Liu, G. Liu and X. Shi, *Coll. Surf. A: Physicochem. Eng. Aspects* 2010, **363**, 35.
67 X.F. Chen, X.C Wang, Y.D. Hou, J.H. Huang, L. Wu and X.Z. Fu, *J. Catal.* 2008, **255**, 59.
68 J.W. Wang, W. Zhu, Y.Q. Zhang and S.X. Liu, *J. Phys. Chem. C* 2007, **111**, 1010.
69 C. Di Valentin, E. Finazzi, G. Pacchioni, A. Selloni, S. Livraghi, M.C. Paganini and E. Giamello, *Chem. Phys.* 2007, **339**, 44.
70 Y. Cong, J.L. Zhang, F. Chen and M. Anpo, *J. Phys. Chem. C* 2007, **111**, 6976.
71 S. Livraghi, M.C. Paganini, E. Giamello, A.;Selloni, C. Di Valentin and G. Pacchioni, *J. Am. Chem. Soc.* 2007, **128**, 15666.
72 E. Wang, P. Zhang, Y. Chen, Z. Liu, T. He and Y. Cao, *J Mater Chem 2012,* **22**, 14443.
73 L. Forss and M. Schubnell, *Appl. Phys. B* 1993, **56**, 363.
74 G. Redmond, D. Fitzmaurice and M. Graetzel, *J. Phys. Chem.* 1993, **97**, 6951.

New Journal of Chemistry Accepted Manuscript

This journal is © The Royal Society of Chemistry [year]

75 J.H. Jang, K.S. Jeon, T.S. Park, K.W. Lee and M. Yoon, *J. Chin. Chem. Soc*. 2006, **53**, 123.
76 S.M. Prokes, J.L. Gole, X. Chen, C. Burda and W.E. Carlos, *Adv. Funct. Mater*. 2005, **15**, 161.
77 J. Li, N. Lu, X. Quan, S. Chen and H. Zhao, *Ind. Eng. Chem. Res.* 2008, **47**, 3804.
78 F. He, F. Ma, T. Li and G. Li, *Chin. J. Catal.* 2013, **34**, 2263.
79 H. Diker, C. Varlikli and E. Stathatos, *Inter. J Energ. Res.* 2014, **38**, 908.
80 J. Ananpattarachai, P. Kajitvichyanukul and S. Seraphin, *J. Hazard. Mater*. 2009, **168**, 253.
81 Y.T. Lin, C.H. Weng, H.J. Hsu, Y.H. Lin and C.C. Shiesh, *Int J Photoenerg,* 2013, id 268723, doi: dx.doi.org/10.1155/2013/268723.
82 X. Cheng, H. Liu, Q. Chen, J. Li and P. Wang, *Electrochim. Acta* 2013, **103**, 134.
83 X. Hou, F. Liu, K. Yao, H. Ma, J. Dong, D. Li and B. Liao, *Mater. Lett*. 2014, **124**, 101.

New Journal of Chemistry Accepted Manuscript